



Phenolic compounds from the leaves of *Cyclocarya paliurus* (Batal.) Ijinskaja and their inhibitory activity against PTP1B

Juan Zhang^{a,c}, Qiang Shen^b, Jin-Cai Lu^c, Jing-Ya Li^b, Wen-Yong Liu^a, Jian-Jun Yang^d, Jia Li^{b,*}, Kai Xiao^{a,*}

^a Lab of Toxicology and Pharmacology, Faculty of Naval Medicine, Second Military Medical University, Shanghai 200433, China

^b National Center for Drug Screening, Shanghai Institute of Materia Medica, Chinese Academy of Sciences, Shanghai 201203, China

^c School of Traditional Chinese Materia Medica, Shenyang Pharmaceutical University, Shenyang 110016, China

^d Jiangxi Xiushui Shencha Co. Ltd., Xiushui, Jiangxi 332400, China

ARTICLE INFO

Article history:

Received 3 June 2009

Received in revised form 24 August 2009

Accepted 8 September 2009

Keywords:

Cyclocarya paliurus

Phenolic compounds

Naphthoquinone derivative

PTP1B inhibitors

Anti-obesity

ABSTRACT

Phenolic compounds were separated from the leaves of *Cyclocarya paliurus* (Batal.) Ijinskaja and their bioactivities were evaluated through an *in vitro* PTP1B inhibitory assay. Bioassay-guided fractionation of the ethanol extract has resulted in the isolation of a naphthoquinone derivative, (1R, 2R, 4R)-1,2,4-trihydroxy-1,2,3,4-tetrahydro-naphthalene-1-O-β-D-glucopyranoside, named cyclonoside A, and a lactone, (4R, 5S, 6R)-8,9,10-trihydroxy-4-[3',4'-dihydroxyphenyl]-1,6-dioxaspiro[4,5]decan-2-one, named cyclospiroside, along with 10 known phenolic compounds: quercetin-3-O-α-D-glucuronide, quercetin-3-O-β-D-glucuronide, myricetin-3-O-β-D-glucuronide, 1-caffeoylquinic acid, 3-caffeoylquinic acid, 4-caffeoylquinic acid, 5-caffeoylquinic acid, caffeic acid, 5-hydroxynaphthalene-1, 4-di-O-β-D-glucopyranoside and piceid. The structures of these compounds were established by means of spectroscopic methods including extensive 2D NMR techniques and chemical evidence. Among all the compounds, **1**, **2**, **4**, **5**, **10** and **11** showed strong inhibition against PTP1B, with IC₅₀ values ranging from 1.922 ± 0.480 to 10.50 ± 2.67 μg/mL. The results suggested that the extract from this plant could be used as a potential source for functional food ingredient with anti-obesity.

© 2009 Elsevier Ltd. All rights reserved.

1. Introduction

In recent years, with increase of intake of foods with high energy, nutritional balance is overlooked and the incidence of obesity and diabetes is increasing at an alarming rate. Reversible tyrosine phosphorylation of cellular proteins plays a pivotal role for the control of a wide range of cellular processes including the maintenance of homeostasis (Alonso et al., 2004). Dephosphorylation of the phosphorylated tyrosine residue of a protein is catalysed by the protein tyrosine phosphatase (PTPase) family of enzymes, which is composed of 107 highly homologous members (Alonso et al., 2004), among which PTP1B is one of the most intensively studied enzymes. There is substantial evidence that PTP1B is the critical point in the insulin signalling pathway (Bialy & Waldmann, 2005; Johnson, Ermolieff, & Jirousek, 2002; Koren & Fantus, 2007; Kraut-Cohen, Muller, & Elson, 2008). The overexpression of PTP1B has been shown to inhibit the increased expression of insulin in insulin-resistant states (Ahmad, Azevedo, Cortright, Dohm, & Goldstein, 1997). Furthermore, recent genetic evidence has shown that PTP1B gene variants are associated with changes in insulin sensi-

tivity (Elchebly et al., 1999). PTP1B could also attenuate leptin pathway, resistance to which is closely associated with obesity (Cheng et al., 2002; Zabolotny et al., 2002). Based on these research results, it has been suggested that components that reduce PTP1B activity or expression levels could be used for treating obesity and diabetes as a functional food ingredient.

Phenolic compounds have shown beneficial bioactivities, such as antioxidant (Peterson & Dwyer, 1998), anticarcinogenic (Bailey & Williams, 1993), antibacterial (Meng, Lozano, Bombarda, Gaydou, & Li, 2008), antimutagenic (Liverio, Puglisi, Morazzoni, & Bombardelli, 1994), anti-inflammatory (Ueda, Yamazaki, & Yamazaki, 2002), antiallergic (Sanbongi et al., 2004), anti-obesity and anti-diabetic activities (Hsu & Yen, 2008). Phenolic compounds, especially flavonoids, in the light of their extremely high values, have become a hot topic for research and development. Consequently, phenolic compounds are not only used as functional food ingredients, but also for other preparations of health-promoting products.

Traditional Chinese medicines are good sources of phenolic compounds and have a long history and are used in the treatment of obesity and diabetes and as a potential source for functional food ingredients. Therefore, we have screened hundreds of plant extracts against this biological target, and the extract of *Cyclocarya paliurus* (Batal.) Ijinskaja showed strong inhibitory activity against PTP1B (IC₅₀ = 1.27 μg/mL). *C. paliurus* belongs to the genus

* Corresponding authors. Tel.: +86 21 50801313x132; fax: +86 21 50801552 (J. Li), tel.: +86 21 81871129; fax: +86 21 81871128 (K. Xiao).

E-mail addresses: jl@mail.shcnc.ac.cn (J. Li), kaixiaocn@gmail.com (K. Xiao).

Cyclocarya (Juglandaceae), which is mainly distributed in southern provinces of China. *C. paliurus* has been used as a traditional tonic and its leaves are processed as tea products in China. Previous chemical studies have reported the presence of abundant phenolic compounds, especially flavonoids, from *Cyclocarya* species (Agerstrand, Ruden, & Wester, 2008; Burge & Manchester, 2008; Li et al., 2008). Thus, it is important to develop *C. paliurus* as a functional food or an ingredient to be used for treatment of diabetes and obesity.

In the present work, water-soluble extract of the leaves of *C. paliurus* was used for bioassay-guided fractionation leading to the isolation of 12 secondary metabolites, two of which were novel structures. The compounds obtained were determined for their inhibitory activity against PTP1B.

2. Materials and methods

2.1. Plant material

The leaves of *C. paliurus* were collected in March 2004 at Xiushui in the Jiangxi Province of China and identified by Jianjun Yang of Jiangxi Xiushui Shenchu Co. Ltd. A voucher specimen has been deposited at Lab of Toxin and Pharm, Faculty of Naval Medicine, Second Military Medical University, Shanghai, China.

2.2. General experimental procedures

All melting points were determined on a SGW X-4 melting point apparatus (Shanghai Huayan Instrument Co. Ltd., Shanghai, China). The UV spectra were obtained on a CARY100 UV-Vis Spectrophotometer (Varian Inc., Palo Alto, CA, USA). The IR spectra were recorded on a Vector 22 Infrared Spectrophotometer (Bruker Corporation, Bremen, Germany). The ^1H , ^{13}C NMR and 2D NMR data (including HMQC, HMBC, NOESY and ^1H - ^1H COSY) were measured on a Bruker AV-500 spectrometer instrument (Bruker Corporation, Bremen, Germany) operating at 500 MHz for ^1H and 125 MHz for ^{13}C . The chemical shifts (δ) are reported in ppm downfield from tetramethylsilane (TMS) using TMS or the solvent signal as standard. The HRESI-TOF-MS and ESI-TOF-MS/MS were obtained on a Q-TOF micromass spectrometer (Waters Corporation, Manchester, England) and LCQ Deca XP Max Liquid Chromatography-Mass (Thermo Scientific Co. Ltd., New York, USA). Analytical thin layer chromatography (TLC) was performed on HSGF₂₅₄ and the spots were detected by ultraviolet irradiation (254 and 365 nm) and by spraying with vanillin-H₂SO₄ reagent.

2.3. Extraction and isolation

The dried leaves (10 kg) of *C. paliurus* were extracted with 70% ethanol under reflux condition three times. The suspension was filtered and the filtrates were concentrated under *in vacuo* to give crude extract (IC₅₀ = 1.27 $\mu\text{g}/\text{mL}$). This residue was subjected to column chromatography on Diaion HP20 macropore polymeric adsorbent (200–600 μm , Japan Mitsubishi Chemical Corporation, Tokyo, Japan), after removing sugar with water elution, using a stepwise gradient of ethanol (10–90%) to give four fractions labelled A (105 g), B (108 g), C (68 g) and D (117 g) according to their TLC profiles. Fraction A (IC₅₀ = 4.10 \pm 0.15 $\mu\text{g}/\text{mL}$) was separated by column chromatography on MCI gel CHP20P (75–150 μm , Japan Mitsubishi Chemical Corporation, Tokyo, Japan), eluted with methanol (10–90%) gradiently to yield three sub-fractions (sub-fractions A-1–A-3). Sub-fraction A-1 was again subject to column chromatography on TSK gel Toyopearl HW40F (30–60 μm , Tosoh Co. Ltd., Tokyo, Japan) and eluted with water to afford compound **10** (36 mg). Sub-fraction A-3 was purified by column chromatography

on TSK gel Toyopearl HW40F and Cosmosil ODS (40–80 μm , Nacalai Tesque Inc., Kyoto, Japan) repeatedly, and eluted with water to afford compounds **6** (35 mg), **7** (25 mg), **8** (24 mg) and **9** (26 mg). Fraction B (IC₅₀ = 2.95 \pm 0.60 $\mu\text{g}/\text{mL}$) was separated by polyamide (80–100 mesh) using a gradient of ethanol (from 10% to 95%), to yield six sub-fractions (sub-fractions B-1–B-6). Further repeated purification of sub-fractions B-2 (78 mg), B-3 (87 mg) and B-5 (67 mg) by column chromatography on TSK gel Toyopearl HW40F, using water as eluant, resulted in the isolation of compounds **3** (24 mg), **4** (15 mg) and **5** (22 mg), respectively. Fraction C (IC₅₀ = 3.57 \pm 0.32 $\mu\text{g}/\text{mL}$) was separated by column chromatography on TSK gel Toyopearl HW40F using a stepwise gradient to yield five sub-fractions (sub-fractions C-1–C-6). Then sub-fractions C-1 and C-2 were purified by repeated column chromatography on TSK gel Toyopearl HW40F and Cosmosil ODS, using water as eluant, to afford compounds **1** (47 mg) and **2** (7 mg). Fraction D (IC₅₀ = 3.47 \pm 0.39 $\mu\text{g}/\text{mL}$) was separated by MCI gel CHP20P, using a gradient of methanol (from 10% to 60%), to give colourless and transparent crystal. Through repeated recrystallization, compound **12** (34 mg) was obtained.

2.3.1. Cyclonoside A (**1**)

Colorless and crystal needles, m.p. 156–157 °C. UV $\lambda_{\text{max}}^{\text{MeOH}}$ nm (log ϵ): 212 (2.30) and 261 (0.07). IR $\nu_{\text{max}}^{\text{MeOH}}$: 3428, 3343, 2922, 2852, 1700, 1651, 1558, 1456, 1379, 1322, 1259, 1162, 1022, 989, 930 and 892 cm^{-1} . ^1H and ^{13}C NMR (see Table 1). ESI-TOF-MS⁺ m/z 365.91 [M+Na]⁺, 707.48 [2M+Na]⁺, 804.89, 533.24, 464.07, 414.22, 360.59, 260.48; ESI-TOF-MS⁻ m/z 341.50 [M-H]⁻, 683.11 [2M-H]⁻, 477.28, 387.34. HRESI-MS m/z 365.1214 (calcd. for C₁₆H₂₂O₈ + Na, 365.1212).

2.3.2. Acid hydrolysis of **1**

About 2 mg of **1** was refluxed in 2 mL 7% HCl–EtOH (3/7) for 4 h. The mixture was diluted with distilled water and extracted with diethyl ether. The aqueous layer was neutralised with 1 M NaOH and subjected to TLC analysis on Kieselgel 60 F₂₅₄ (Merck Chemical Co. Ltd., Darmstadt, Germany) [using CHCl₃–MeOH–H₂O (15/6/2), 9 mL and HOAc, 1 mL] and paper chromatography [using *n*-BuOH–HOAc–H₂O (4/1/5)] with standard sugars, in this case the presence of glucose was established. The aqueous layer was then passed through an Amberlite IRA-60E column (Sigma–Aldrich Co. Ltd., St. Louis, MO, USA), and the aqueous eluate was concentrated and treated with thiazolidine. Only the D -glucose derivative was detected by GC (GC conditions: column, Supelco SPB⁻¹,

Table 1

^1H NMR (500 MHz, DMSO-*d*₆ + D₂O), ^1H NMR (500 MHz, DMSO-*d*₆) and ^{13}C NMR (125 MHz, DMSO-*d*₆ + D₂O) of compound **1**.

No.	δ_{H} (DMSO- <i>d</i> ₆ + D ₂ O)	δ_{H} (DMSO- <i>d</i> ₆)	δ_{C}
1	4.41 (1H, d, <i>J</i> = 6.3)	4.40 (1H, d, <i>J</i> = 6.3)	82.7 (d)
2	4.08 (1H, m)	4.07 (1H, m)	67.1 (d)
3 α	1.91 (1H, m)	1.90 (1H, m)	36.6 (t)
3 β	2.00 (1H, m)	1.99 (1H, m)	
4	4.69 (1H, t-like, <i>J</i> = 5.1)	4.68 (1H, q-like, <i>J</i> = 5.2)	65.1 (d)
5	7.38 (1H, br d, <i>J</i> = 7.3)	7.37 (1H, br d, <i>J</i> = 7.3)	128.0 (d)
6	7.27 (1H, dt, <i>J</i> = 7.3, 1.3)	7.26 (1H, dt, <i>J</i> = 7.3, 1.2)	127.6 (d)
7	7.23 (1H, dt, <i>J</i> = 7.3, 1.3)	7.21 (1H, dt, <i>J</i> = 7.3, 1.2)	127.2 (d)
8	7.67 (1H, br d, <i>J</i> = 7.3)	7.68 (1H, br d, <i>J</i> = 7.3)	128.9 (d)
9	–	–	134.9 (s)
10	–	–	139.7 (s)
1'	4.45 (1H, d, <i>J</i> = 7.8)	4.44 (1H, d, <i>J</i> = 7.8)	103.6 (d)
2'	3.10 (1H, m)	3.08 (1H, m)	73.8 (d)
3'	3.20 (1H, m)	3.18 (1H, m)	76.9 (d)
4'	3.20 (1H, m)	3.18 (1H, m)	70.3 (d)
5'	3.10 (1H, m)	3.08 (1H, m)	76.8 (d)
6' α	3.75 (1H, dd, <i>J</i> = 11.6, 1.5)	3.74 (1H, m)	61.2
6' β	3.46 (1H, dd, <i>J</i> = 11.6, 6.7)	3.45 (1H, m)	

0.25 mm × 27 m (Sigma–Aldrich Co. Ltd., St. Louis, MO, USA), column temperature 230 °C; carrier gas, N₂; *t*_R, D-glucose derivative 17.9 min, L-glucose derivative 17.3 min).

2.3.3. Cyclospiroside (2)

Amorphous powder, m.p. 156–157 °C. UV $\lambda_{\max}^{\text{MeOH}}$ nm (log ϵ): 205 (1.82) and 282 (0.23). IR ν_{\max}^{MeOH} : 3479, 3425, 3194, 3038, 2984, 2931, 2898, 1805, 1787, 1677, 1604, 1279, 1260, 1222, 1200, 1137, 1122, 1075, 1052, 1028 and 967 cm⁻¹. ¹H and ¹³C NMR (see Table 2). ESI-TOF-MS⁻ *m/z* 311.36 [M–H]⁻, 623.32 [2M–H]⁻, 679.45, 401.14, 347.16, 221.33, 177.36. HRESI-MS *m/z* 312.0827 (calcd. for C₁₄H₁₆O₈, 312.0845).

2.4. Bioactivity assay

2.4.1. PTP1B enzymatic assay

PTP1B (human, recombinant) was expressed and purified, and the enzyme activity was measured at 30 °C by monitoring the hydrolysis of pNPP (Zhang et al., 2006). The enzymatic activities of PTP1B catalytic domain were determined at 30 °C by monitoring the hydrolysis of pNPP. Dephosphorylation of pNPP generates product pNP, which can be monitored at 405 nm. In a typical 100 μ L assay mixture containing 50 mM MOPS, pH 6.5, 2 mM pNPP and recombinant enzymes, PTP1B activities were continuously monitored and the initial rate of the hydrolysis was determined using the early linear region of the enzymatic reaction kinetic curve.

2.4.2. PTP1B inhibition screening

The samples were screened against the PTP1B with the colorimetric assay. The high-throughput screening system of PTP1B was similar with LAR (Zhang et al., 2006). Briefly, the samples were solubilised in dimethyl sulphoxide at 5 mg/mL, and 2 μ L samples were distributed to A2–H11 wells of 96-well clear polystyrene plate (Corning, Action, MA). The dimethyl sulphoxide (2 μ L) was distributed to A1–D1 and E12–H12 wells as the full enzyme activity, and orthovanadate (12.5 mM, 2 μ L) was distributed to E1–H1 and A12–D12 wells as the positive inhibition. After adding an assay mixture (88 μ L), 10 μ L of the GST-PTP1B (300 nM) were added to initiate the reaction. The high-throughput screening was carried out in a final 100 μ L volume containing 50 mM MOPS, pH 6.5, 2 mM pNPP, 30 nM PTP1B and 2% dimethyl sulphoxide, and the catalysis of pNPP was continuously monitored on SpectraMax 340 microplate reader (Molecular Devices Corporation, Sunnyvale, USA) at 405 nm for 2 min at 30 °C.

Table 2

¹H NMR (500 MHz, DMSO-*d*₆ + D₂O), ¹³C NMR (500 MHz, DMSO-*d*₆) and ¹³C NMR (125 MHz, DMSO-*d*₆ + D₂O) of compound 2.

No.	δ_{H} (DMSO- <i>d</i> ₆ + D ₂ O)	δ_{H} (DMSO- <i>d</i> ₆)	δ_{C}
2	–	–	175.3 (s)
3 α	2.68 (1H, dd, <i>J</i> = 9.2, 17.8)	2.63 (1H, dd, <i>J</i> = 9.0, 17.8)	36.6 (t)
3 β	2.96 (1H, dd, <i>J</i> = 9.2, 17.8)	2.95 (1H, dd, <i>J</i> = 9.0, 17.8)	
4	3.74 (1H, t, <i>J</i> = 9.2)	3.72 (1H, t, <i>J</i> = 9.0)	46.6 (d)
5	–	–	109.2 (s)
7 α	3.27 (1H, t, <i>J</i> = 9.8)	3.25 (1H, t, <i>J</i> = 9.6)	65.8 (t)
7 β	3.62 (1H, dd, <i>J</i> = 5.3, 9.8)	3.58 (1H, overlapped)	
8	3.57 (1H, dd, <i>J</i> = 5.4, 9.4)	3.58 (1H, overlapped)	65.5 (d)
9	3.51 (1H, dd, <i>J</i> = 2.5, 9.4)	3.49 (1H, br s)	71.6 (d)
10	3.79 (1H, overlapped)	3.77 (1H, br.s)	72.9 (d)
1'	–	–	117.4 (d)
2'	6.71 (1H, s)	6.68 (1H, s)	144.4 (s)
3'	–	–	144.2 (s)
4'	–	–	115.1 (d)
5'	6.62 (1H, d, <i>J</i> = 8.0)	6.64 (1H, d, <i>J</i> = 8.0)	121.6 (d)
6'	6.57 (1H, d, <i>J</i> = 8.0)	6.61 (1H, d, <i>J</i> = 8.0)	129.2 (s)

For calculating IC₅₀, inhibition assays were performed with 30 nM recombinant enzyme, 2 mM pNPP in 50 mM MOPS at pH 6.5 and the inhibitors diluted around the estimated IC₅₀ values. IC₅₀ was calculated from the non-linear curve fitting of per cent inhibition (% inhibition) vs. inhibitor concentration *I* by using the following equation:

$$\% \text{ Inhibition} = 100 / \{1 + (\text{IC}_{50} / [I])^k\}$$

where *k* is the Hill coefficient.

2.5. Statistical analysis

For bioactivity assay, all determinations were triplicates, and mean values and standard deviations were calculated. Analysis of variance (ANOVA) was performed and the mean separation was done by LSD (*P* ≤ 0.05) using SPSS 13.0 program for windows (SPSS Inc., IL, USA).

3. Results and discussion

3.1. Extraction and isolation

Bioactivity-guided fractionation of the water-soluble extract of *C. paliurus*, using an *in vitro* PTP1B inhibitory assay, led to the isolation and characterisation of a new naphthoquinone derivative, named cyclonoside A (1), and a new lactone named cyclospiroside (2), along with 10 known secondary metabolites (3–12). The known compounds were identified by comparison of their physico-chemical and spectroscopic data (¹H, ¹³C NMR, 2D NMR and MS) with those of authentic samples and reference data as: quercetin-3-O- α -D-glucuronide (3), quercetin-3-O- β -D-glucuronide (4), myricetin-3-O- β -D-glucuronide (5) (Loke et al., 2008; Nakanishi et al., 2007), 1-caffeoylquinic acid (6), 3-caffeoylquinic acid (7), 4-caffeoylquinic acid (8), 5-caffeoylquinic acid (9), caffeic acid (10) (Liu et al., 2009; Zhou et al., 2009), 5-hydroxynaphthalene-1, 4-di-O- β -D-glucopyranoside (11) (Liu, Li, Koike, & Nikaido, 2004) and piceid (12) (Fig. 1) (Jayatilake et al., 1993).

3.2. Structure determination of compound 1

Compound 1, m.p. 155–157 °C, was obtained as colourless and crystal needles from a 10% ethanol solution. It showed positive results in Molish test, suggesting the presence of sugar moiety in the molecule. Its molecular formula was determined to be C₁₆H₂₂O₈ using positive high-resolution electrospray ionisation time of flight (HR-ESI-TOF) mass spectroscopy which showed a quasi-molecular ion [M+Na]⁺ peak at *m/z* 365.1214 (calcd. for C₁₆H₂₂O₈Na, 365.1212). The ESI-MS spectrum in negative ion mode exhibited the quasi-molecular ion [M–H]⁻ peak at *m/z* 341.50 and ion [2M–H]⁻ peak at *m/z* 683.11. The IR spectrum of compound 1 displayed the presence of hydroxyl group (ν_{\max} 3343.45–3428.33 cm⁻¹) and aromatic ring (ν_{\max} 1455.17–1558.94 cm⁻¹) (Wang, Liu, Liu, Zhang, & Xian, 2008), which was also evidenced by the UV spectrum [λ_{\max} (log ϵ): 261 (0.07) nm]. The ¹H NMR spectrum (DMSO-*d*₆ + D₂O) (Table 1) of compound 1 exhibited two double doublets at δ_{H} 7.67 (1H, dd, *J* = 7.3, 1.3 Hz) and δ_{H} 7.38 (1H, dd, *J* = 7.3, 1.3 Hz) and two double triplets at δ_{H} 7.27 (1H, dt, *J* = 7.3, 1.3 Hz), δ_{H} 7.23 (1H, dt, *J* = 7.3, 1.3 Hz), which were assignable to a 1,2-disubstituted benzene ring with the assistance from the analysis of HMBC (Fig. 2A1) and HMQC experiments. The ¹³C NMR spectrum (Table 1) of compound 1 revealed 16 carbon signals as two methylenes, 12 methines and two quaternary carbons assignable to one benzene ring, one glucose, three oxygenated sp carbons and one sp² carbon. Full analysis of the COSY, HMBC and HMQC spectra led to the identification of a 1,2,3,4-tet-

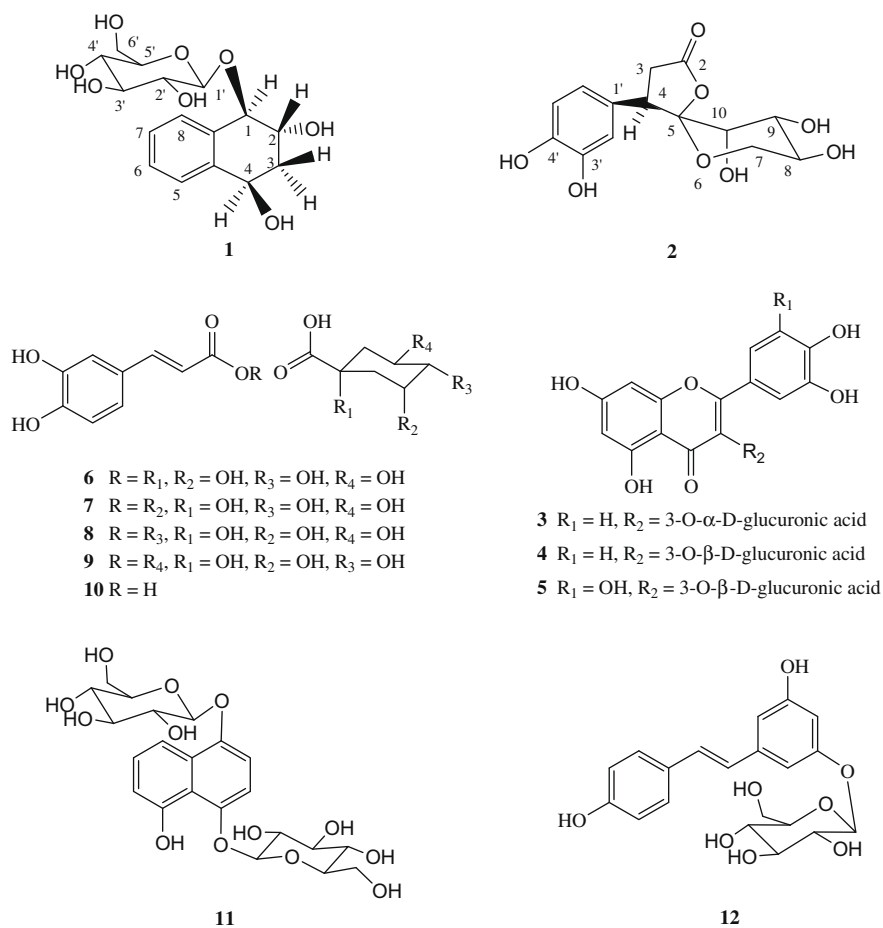


Fig. 1. Chemical structures of compounds 1–12.

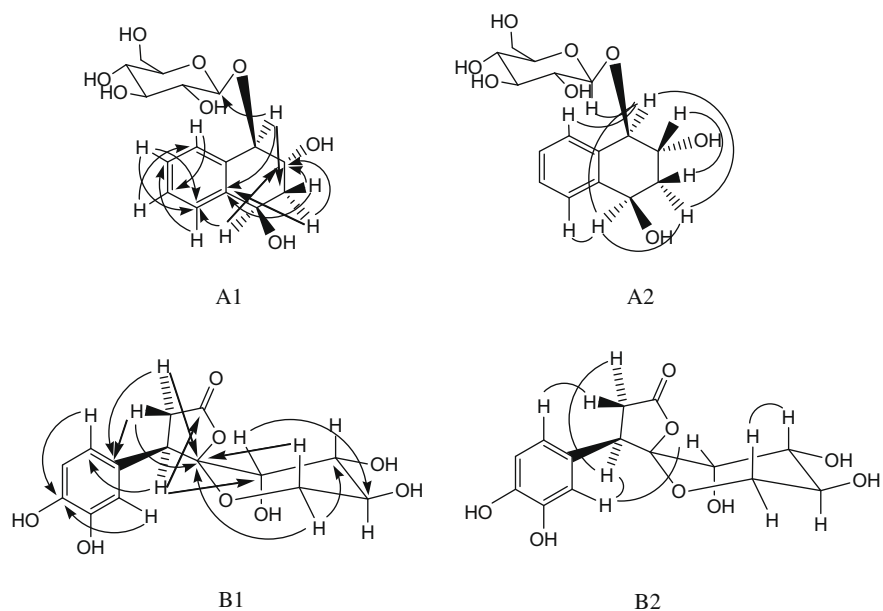


Fig. 2. Significant HMBC (1) and NOESY (2) correlations of compound 1 (A1 and A2) and 2 (B1 and B2).

rahydronaphthalene skeleton as shown in Fig. 1. The ^{13}C NMR pattern of the sugar moiety was characteristic of a glucose (Agrawal, 1992) and was further determined as D -glucose according to the results of the acidic hydrolysis and the subsequent GC analysis (Miy-

ase, Saitoh, Shiokawa, & Ueno, 1995). In the HMBC of compound 1, the significant correlations between $H'-1$ (δ 4.45) and $C-1$ (δ 82.7), $H-1$ (δ 4.41) and $C-1$ (δ 103.6) indicated that the glucose was attached to $C-1$, and the β -linkage of the glucose was determined

from the coupling constant of the anomeric proton ($J = 7.8$ Hz) (Agrawal, 1992). A combination analysis of the HMQC, HMBC and ^1H - ^1H COSY experiments allowed the unambiguous assignment of all the signals (Table 1). Moreover, in the NOESY spectrum of compound **1**, strong correlations between H-3 α (δ 1.91) and H-4 (δ 4.69), and between H-3 β (δ 2.00) and H-2 (δ 4.08) showed that H-1, H-3 α and H-4 located at the same side of the planar, while H-2 and H-3 β located at the opposite side (Fig. 2A2).

Finally, the structure and stereochemistry of compound **1** were further established by means of X-ray single-crystal crystallography analysis (Fig. 3). Crystal data of compound **1** was exhibited as follows: $\text{C}_{16}\text{H}_{24}\text{O}_9$ (co-crystallized with one H_2O molecules), M_r 360.35, monoclinic, space group $P2_1$, $a = 8.1569(10)$ Å, $b = 12.4319(15)$ Å, $c = 8.3561(10)$ Å, $\beta = 100.559(2)^\circ$, $V = 833.01(17)$ Å³, $Z = 2$, $D_c = 1.437$ Mg m⁻³, $F(000) = 536$, $\lambda = 0.71073$ Å, $\mu = 0.118$ mm⁻¹. Data were collected from a $0.20 \times 0.15 \times 0.15$ mm³ crystal on a Bruker SMART APEX CCD area detector diffractometer at 296(2) K. A total of 5225 reflections were collected for $2.48^\circ < \theta < 27.00^\circ$ and $-10 \leq h \leq 9$, $-12 \leq k \leq 15$, $-10 \leq l \leq 10$. There were 1904 independent reflections. Semi-empirical absorption correction from equivalents was applied. The structure was solved by means of direct method with SHELXS-97 to final indices $R [F^2 > 2\sigma(F^2)]: 1904$ reflections = 0.0293 and $wR(F^2) = 0.0740$, $[w = 1/(\sigma^2(F_o^2) + (0.053P)^2)]$, where $P = (Fo^2 + 2Fc^2)/3$. The hydrogen atoms were placed in calculated positions and added to the refinement as a fixed isotropic contribution. The goodness-of-fit on F^2 was 1.057, and the last residual Fourier positive and negative peaks were equal to 0.196 and -0.198 , respectively. Crystallographic data (excluding structure factors) for the structure in this paper have been deposited with the Cambridge Crystallographic Data Centre as supplementary publication numbers CCDC 721236. Copies of the data can be obtained free of charge on application to CCDC, Cambridge, UK. Since the absolute configuration of the sugar has been established, the absolute structure of compound **1** has also resolved in the X-ray analysis. On the basis of the above results, the structure of compound **1** was determined to be (1*R*, 2*R*, 4*R*)-1,2,4-trihydroxy-1,2,3,4-tetrahydro-naphthalene-1-*O*- β -*D*-glucopyranoside, named cyclonside A.

3.3. Structure determination of compound **2**

Compound **2**, m.p. 291–292 °C, was obtained as amorphous powder from a 10% ethanol solution. Its molecular formula was

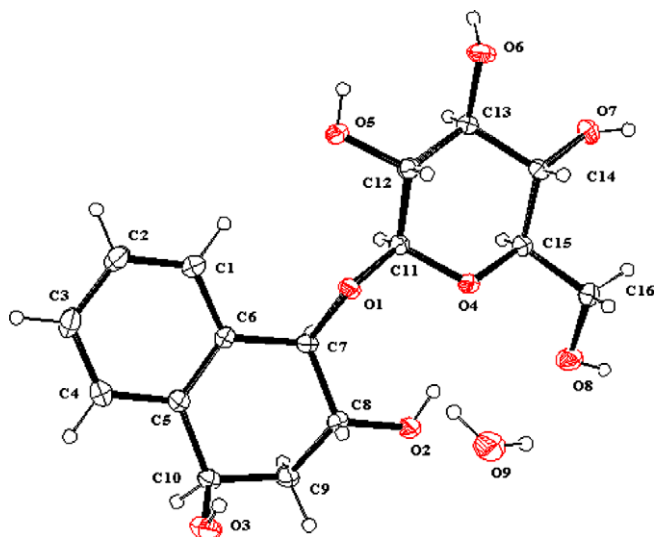


Fig. 3. ORTEP drawing of compound **1**.

determined to be $\text{C}_{14}\text{H}_{16}\text{O}_8$ as evidenced by HR-ESI-TOF mass spectroscopy which showed a molecular ion $[\text{M}]^+$ peak at m/z 312.0827 (calcd. for $\text{C}_{14}\text{H}_{16}\text{O}_8$, 312.0845). The ESI-MS spectrum in negative ion mode showed the quasi-molecular ion $[\text{M}-\text{H}]^-$ peak at m/z 311.36 and ion $[2\text{M}-\text{H}]^-$ peak at m/z 623.32. The IR spectrum of **2** suggested the presence of hydroxyl group (ν_{max} 3194.24–3479.68 cm^{-1}), carbonyl group (ν_{max} 1787 cm^{-1}) and aromatic ring (ν_{max} 1416.78–1604.25 cm^{-1}). The UV spectrum also suggested the existence of benzene ring and carbonyl group in compound **2** [λ_{max} ($\log \epsilon$): 282 (0.24) nm] (Kenawi, Barsoum, & Youssef, 2005). In the ^1H NMR spectrum (DMSO- d_6 + D_2O) (Table 2) of **2**, an ABC spin system, resonating at δ_{H} 6.62 (1H, d, $J = 8.0$ Hz), 6.57 (1H, d, $J = 8.0$ Hz) and 6.71 (1H, s), could be attributed to a 1,3,4-trisubstituted benzene ring. The ^{13}C NMR spectrum (Table 1) of compound **2** showed 14 carbon signals as two methylenes, seven methines and five quaternary carbons, among which one carbonyl group (δ 175.3), one benzene ring and five oxygen-bearing carbons [δ 65.5 (d), 65.8 (t), 71.6 (d), 72.9 (d) and 109.2 (s)] could be assigned. Though compound **2** exhibited some resemblance to the NMR pattern of sugar moiety, negative result in Molish test excluded the presence of sugar moiety in the molecule. In addition of the benzene ring, full analysis of the ^1H , ^{13}C NMR, COSY, HMBC and HMQC spectra revealed the presence of one γ -butyrolactone group [δ_{H} 3.74/ δ_{C} 46.6 (1H, t, $J = 9.2$), two double doublets at δ_{H} 2.96/ δ_{C} 36.6 (1H, dd, $J = 9.2, 17.8$), δ_{H} 2.68/ δ_{C} 36.6 (1H, dd, $J = 9.2, 17.8$), δ_{C} 175.3 and 109.2], one saturated trihydroxypyran ring moiety and one lactol ether linkage, which formed 1,6-dioxaspiro[4,5]decan-2-one as the skeleton of compound **2**. Analysis of the ^1H - ^1H COSY, HMBC and HMBC experiment results permitted the full assignment of the signals (Table 2). Furthermore, the coupling constants of proton signals on the trihydroxypyran ring demonstrated that the hydroxyl groups of compound **2** were axially-oriented at C-10 and equatorial at C-9 and C-8 in a chair conformation. In the NOESY spectrum of **2**, significant correlations between H-4 (δ 3.74) and H-3 α (δ 2.96), between H-9 (δ 3.51) and H-7 β (δ 3.27) showed that H-4 and H-3 α located at the same planar of the γ -butyrolactone ring, and H-9 and H-7 β located at the same planar of the saturated trihydroxypyran ring, respectively (Fig. 2B2). It turned out that compound **2** was a derivative of sawaranospirolide D. Compared to sawaranospirolide D reported by Hasegawa et al. (1990), the benzene ring of **2** possessed one more additional hydroxyl group, and the rest parts of compound **2** were in agreement with sawaranospirolide D. On the basis of the results described above, the structure of compound **2** was determined to be (4*R*, 5*S*, 6*R*)-8, 9, 10-trihydroxy-4-[3',4'-dihydroxyphenyl]-1,6-dioxaspiro[4,5]decan-2-one (Fig. 1), named cyclospiroside.

3.4. Determination of inhibitory activity against PTP1B

PTP1B (human, recombinant) was expressed and purified, and the enzyme activity was measured using *p*-nitrophenyl phosphate (*p*NPP) as a substrate (Burke et al., 1996). All the isolates were assayed for their inhibitory activity against PTP1B, and the results were presented in Table 3. The known PTP1B inhibitor HD0518 was used as positive controls in this assay. The bioactivity in the total extract was higher than in any fraction obtained using 10–90% ethanol as eluent, suggesting that interaction effect among different compounds might contribute to inhibitory effect against PTP1B. Six compounds inhibited PTP1B activity in a dose-dependent manner. Of the compounds tested, **1** and **10** exhibited the most potent inhibitory activities, with IC_{50} values of 2.11 ± 0.66 and 1.922 ± 0.480 $\mu\text{g}/\text{mL}$, respectively.

Compound **5** ($\text{IC}_{50} = 9.47 \pm 3.31$ $\mu\text{g}/\text{mL}$), with one more hydroxyl group substituted at C-5', was a little less active than compound **4** ($\text{IC}_{50} = 7.39 \pm 1.15$ $\mu\text{g}/\text{mL}$), indicating that addition of one hydroxyl group to C-5' in the B ring may be responsible for

Table 3
Inhibitory activity of different fractions and compounds 1–12 against PTP1B.

Fraction	IC ₅₀ (μg/mL) ^{A,B,C}	Compounds	IC ₅₀ (μg/mL) ^{A,B,C}
Total extract	1.27 ± 0.12 ^a	1	2.11 ± 0.66 ^a
Fraction A	4.10 ± 0.15 ^b	2	16.64 ± 0.04 ^b
Fraction B	2.95 ± 0.60 ^c	4	7.39 ± 1.15 ^c
Fraction C	3.57 ± 0.32 ^d	5	9.47 ± 3.31 ^a
Fraction D	3.47 ± 0.39 ^e	10	1.922 ± 0.480 ^d
		11	10.50 ± 2.67 ^e

Means within columns with different superscripts were significantly different ($P \leq 0.05$).

^A IC₅₀ values were determined by regression analyses and expressed as mean ± SD of three replicates.

^B Compounds 3–9 were inactive.

^C Positive control HD0518 with IC₅₀ value of 1.12 ± 0.18 μg/mL.

the decrease of activity *in vitro*. Compound **3**, with different configuration of glucuronic acid moiety compared with **4**, was inactive, implying that the sugar configuration played a key role in the inhibitory activity *in vitro*. Compound **10**, with part molecular structure of inactive compounds **6–9**, showed strong inhibitory activities, suggesting that the free carboxyl group in caffeic acid was vital for the inhibitory activity, while the quinic acid group did not contribute to the activity. Both compounds **1** and **11** belong to naphthoquinone derivatives, revealed strong inhibitory activities. The PTP1B inhibitory activity of the compounds from *C. paliurus* may contribute to the hypoglycaemic effect of this plant and this study, therefore, partly explains the hypoglycaemic mechanism of the plant.

4. Conclusions

Water-soluble extract of *C. paliurus* exhibited strong inhibitory activity against PTP1B (IC₅₀ = 1.27 μg/mL), so it could be used as a potential source for hypoglycaemic and anti-obesity functional food. In the extract, both the naphthoquinone derivatives and phenol–acidic compounds can be considered as promising classes of PTP1B inhibitors. Undoubtedly, this study will provide fundamental knowledge for research and development of *C. paliurus* leaves. In addition, further investigation and optimisation of these derivatives might enable the preparation of new PTP1B inhibitors as a functional food ingredient in the prevention and treatment of diabetes and obesity.

Acknowledgements

The authors are grateful to the financial support from the National Natural Science Foundation of China (20872179 and 30472141), Science and Technology Commission of Shanghai Municipality (STCSM) (08DZ1971504), Shanghai-SK Development Fund (2004005-t) and the Innovation Fund for Graduate Student of Shanghai Jiao Tong University.

References

Agerstrand, M., Ruden, C., & Wester, M. (2008). The Swedish environmental information and classification scheme for pharmaceuticals – An empirical investigation of the motivations, intentions and expectations underlying its development and implementation. *Toxicology Letters*, *180*, S177–S178.

Agrawal, P. K. (1992). NMR spectroscopy in the structural elucidation of oligosaccharides and glycosides. *Phytochemistry*, *31*, 3307–3330.

Ahmad, F., Azevedo, J. L., Cortright, R., Dohm, J. L., & Goldstein, B. J. (1997). Alterations in skeletal muscle protein-tyrosine phosphatase activity and expression in insulin-resistant human obesity and diabetes. *Journal of Clinical Investigation*, *100*, 449–458.

Alonso, A., Sasin, J., Bottini, N., Friedberg, I., Friedberg, I., Osterman, A., et al. (2004). Protein tyrosine phosphatases in the human genome. *Cell*, *117*(6), 699–711.

Bailey, G. S., & Williams, D. E. (1993). Potential mechanisms for food related carcinogens and anti-carcinogens. *Food Technology*, *47*, 105–118.

Bialy, L., & Waldmann, H. (2005). Inhibitors of protein tyrosine phosphatases: Next-generation drugs? *Angewandte Chemie, International Edition in English*, *44*(25), 3814–3839.

Burge, D. O., & Manchester, S. R. (2008). Fruit morphology, fossil history, and biogeography of *paliurus* (rhamnaceae). *International Journal of Plant Sciences*, *169*(8), 1066–1085.

Burke, T. R., Ye, J. B., Yan, X., Wang, S., Jia, Z., Chen, L., et al. (1996). Small molecule interactions with protein-tyrosine phosphatase PTP1B and their use in inhibitor design. *Biochemistry*, *35*(50), 15989–15996.

Cheng, A., Uetani, N., Simoncic, P. D., Chaubey, V. P., Lee-Loy, A., McGlade, C. J., et al. (2002). Attenuation of leptin action and regulation of obesity by protein tyrosine phosphatase 1B. *Developmental Cell*, *2*(4), 497–503.

Elchebly, M., Payette, P., Michaliszyn, E., Cromlish, W., Collins, S., Loy, A. L., et al. (1999). Increased insulin sensitivity and obesity resistance in mice lacking the protein tyrosine phosphatase-1B gene. *Science*, *283*, 1544–1548.

Hasegawa, S., Koyanagi, H., & Hirose, Y. (1990). Decarboxylated ascorbigenes in the heartwood of *Chamaecyparis pisifera*. *Phytochemistry*, *29*(1), 261–266.

Hsu, C. L., & Yen, G. C. (2008). Phenolic compounds: Evidence for inhibitory effects against obesity and their underlying molecular signaling mechanisms. *Molecular Nutrition and Food Research*, *52*, 53–61.

Jayatilake, G., Jayasuriya, H., Lee, E. S., Koonchanok, N. M., Geahlen, R. L., Ashendei, C. L., et al. (1993). Kinase inhibitors from *Polygonum cuspidatum*. *Journal of Natural Products*, *56*, 1805–1810.

Johnson, T. O., Ermolieff, J., & Jirousek, M. R. (2002). Protein tyrosine phosphatase 1B inhibitors for diabetes. *Nature Reviews Drug Discovery*, *1*(9), 696–709.

Kenawi, I. M., Barsoum, B. N., & Youssef, M. A. (2005). Drug–drug interaction between diclofenac, cetirizine and ranitidine. *Journal of Pharmaceutical and Biomedical*, *37*(4), 655–661.

Koren, S., & Fantus, I. G. (2007). Inhibition of the protein tyrosine phosphatase PTP1B: Potential therapy for obesity, insulin resistance and type-2 diabetes mellitus. *Best Practice and Research Clinical Endocrinology and Metabolism*, *21*(4), 621–640.

Kraut-Cohen, J., Muller, W. J., & Elson, A. P. (2008). Protein-tyrosine phosphatase epsilon regulates Shc signaling in a kinase-specific manner – Increasing coherence in tyrosine phosphatase signaling. *Journal of Biological Chemistry*, *283*(8), 4612–4621.

Li, J., Lu, Y. Y., Su, X. J., Li, F., She, Z. G., He, X. C., et al. (2008). A nor-sesquiterpene lactone and a benzoic acid derivative from the leaves of *Cyclocarya paliurus* and their glucosidase and glycogen phosphorylase inhibiting activities. *Planta Medica*, *74*(3), 287–289.

Liu, L., Li, W., Koike, K., & Nikaido, T. (2004). Two new naphthalenyl glucosides and a new phenylbutyric acid glucoside from the fruit of *Juglans mandshurica*. *Heterocycles*, *6*(63), 1429–1436.

Liu, L. Y., Sun, Y., Lauraa, T., Liang, X. F., Ye, H., & Zeng, X. X. (2009). Determination of polyphenolic content and antioxidant activity of kudingcha made from *Ilex kudingcha* C.J. Tseng. *Food Chemistry*, *112*(1), 35–41.

Liverio, L., Puglisi, P. P., Morazzoni, P., & Bombardelli, E. (1994). Antimutagenic activity of procyanidins from *Vitis vinifera*. *Journal for the Study of Medicinal Plants*, *65*, 203–209.

Loke, W. M., Proudfoot, J. M., Mckinley, A. J., Needs, P. W., Kroon, P. A., Hodgson, J. M., et al. (2008). Quercetin and its *in vivo* metabolites inhibit neutrophil-mediated low-density lipoprotein oxidation. *Journal of Agricultural and Food Chemistry*, *56*(10), 3609–3615.

Meng, L., Lozano, Y., Bombarda, I., Gaydou, E. M., & Li, B. (2008). Polyphenol extraction from eight *Perilla frutescens* cultivars. *Comptes Rendus Chimie*, *1–10*.

Miyase, T., Saitoh, H., Shiokawa, K., & Ueno, A. (1995). Six new presenegenin glycosides, reinosides A–F, from *Polygala reinii* root. *Chemical and Pharmaceutical Bulletin*, *43*, 466–472.

Nakanishi, T., Inatomi, Y., Murata, H., Ishida, S. S., Fujino, Y., Miura, K., et al. (2007). Triterpenes and flavonol glucuronides from *Oenothera cheiranthifolia*. *Chemical and Pharmaceutical Bulletin*, *55*(2), 334–336.

Peterson, J., & Dwyer, J. (1998). Flavonoids: Dietary occurrence and biochemical activity. *Nutrition Research*, *18*, 1995–2018.

Sanbongi, C., Takano, H., Osakabe, N., Sasa, N., Natsume, M., Yanagisawa, R., et al. (2004). Rosmarinic acid in perilla extract inhibits allergic inflammation induced by mite allergen, in a mouse model. *Clinical and Experimental Allergy*, *34*, 971–977.

Ueda, H., Yamazaki, C., & Yamazaki, M. (2002). Luteolin as an anti-inflammatory and anti-allergic constituent of *Perilla frutescens*. *Biological and Pharmaceutical Bulletin*, *25*, 1197–1202.

Wang, H. H., Liu, B., Liu, X. Q., Zhang, J. W., & Xian, M. (2008). Synthesis of biobased epoxy and curing agents using rosin and the study of cure reactions. *Green Chemistry*, *10*(11), 1190–1196.

Zabolotny, J. M., Bence-Hanulec, K. K., Stricker-Krongrad, A., Haj, F., Wang, Y., Minokoshi, Y., et al. (2002). PTP1B regulates leptin signal transduction *in vivo*. *Developmental Cell*, *2*(4), 489–495.

Zhang, W., Hong, D., Zhou, Y. Y., Zhang, Y. N., Shen, Q., Li, J. Y., et al. (2006). Ursolic acid and its derivative inhibit protein tyrosine phosphatase 1B, enhancing insulin receptor phosphorylation and stimulating glucose uptake. *Biochimica et Biophysica Acta*, *1760*, 1505–1512.

Zhou, S. H., Fang, Z. X., Lü, Y., Chen, J. C., Liu, D. H., & Ye, X. Q. (2009). Phenolics and antioxidant properties of bayberry (*Myrica rubra* Sieb. et Zucc.) pomace. *Food Chemistry*, *112*(2), 394–399.